International Journal of Heat and Mass Transfer 52 (2009) 4956–4965

Contents lists available at ScienceDirect

International Journal of Heat and Mass Transfer

journal homepage: www.elsevier.com/locate/ijhmt

Heat transfer in the MHD flow of a power law fluid over a non-isothermal stretching sheet

K.V. Prasad [a], K. Vajravelu [b,*]

[a] Department of Mathematics, Central College Campus, Bangalore University, Bangalore 560001, India
[b] Department of Mathematics, University of Central Florida Orlando, FL 32816, USA

ARTICLE INFO

Article history:
Received 9 February 2009
Received in revised form 14 May 2009
Accepted 14 May 2009
Available online 3 July 2009

Keywords:
Power law fluid
Similarity solution
MHD flow
Variable thermal conductivity
Stretching sheet

ABSTRACT

The article examines the hydromagnetic laminar boundary layer flow and heat transfer in a power law fluid over a stretching surface. The flow is influenced by linear stretching of the sheet. Also the energy equation with temperature-dependent thermal conductivity, thermal radiation, work done by stress, viscous dissipation and internal heat generation is considered. The governing partial differential equations along with the boundary conditions are first cast into a dimensionless form and then the equations are solved by Keller–Box method. The effects of various physical parameters on the flow and heat transfer characteristics are presented graphically and discussed.

1. Introduction

From a technological point of view, non-linear fluid rheology is of special interest and has practical applications. Hence the study of non-Newtonian fluid flow is important. Different models have been proposed to explain the behavior of non-Newtonian fluids. Among these, the power law, the differential type, and the rate type models gained importance. Also boundary layer assumptions were successfully applied to these models.

Flows due to a continuously moving surface are encountered in several process of thermal and moisture treatment of materials, predominantly in processes involving continuous pulling of a sheet through a reaction zone; as in metallurgy, in textiles and paper industries, and in the manufacture of glass sheets and crystalline materials. Also many metallurgical processes involve the cooling of continuous stripes or filaments by drawing them through a quiescent fluid, and in the process of drawing, these strips are stretched. This type of flow was first initiated by Sakiadis [1] for moving an inextensible sheet and later extended by Crane [2] to fluid flow over a linearly stretched sheet.

Thereafter, numerous investigations were made on the stretching sheet problem with linear stretching in different directions [3–8]. All the above studies restrict their analyses to Newtonian flows in the absence of a magnetic field. In recent years, it has been observed that a number of industrial fluids such as molten plastics, artificial fibers, polymeric liquids, blood, food stuff, and slurries exhibit non-Newtonian fluid behavior. It may also be pointed out that, many industrial processes involve the cooling of continuous strips or filaments by drawing them through a quiescent fluid. During this process, these strips are sometimes stretched. Mention may be made of annealing and thinning of copper wires. In all these cases, the properties of the final product depend to a great extent on the rate of cooling. By drawing such strips in an electrically conducting fluid subjected to a uniform magnetic field, the rate of cooling can be controlled and the desired characteristics of the final product can be obtained. Another important application of hydromagnetic flows to metallurgy lies in the purification of molten metals from non-metallic inclusion by the application of magnetic field. In view of these applications, Sarpakaya [9] was the first among others to study the magneto-hydrodynamic flow of non-Newtonian fluids. This work was later extended by many authors by considering the non-Newtonian visco-elastic flow, heat and mass transfer under different physical situations [10–16]. It is worth mentioning here that many inelastic non-Newtonian fluids encountered in chemical engineering processes, are known to follow the empirical Ostwald–de Waele or so called "power law model". This model is described by a simple non-linear equation of state for inelastic fluids which includes linear Newtonian fluids as a special case.

The power law model provides an adequate representation of many non-Newtonian fluids over the most important range of shear stress. Although this model is merely an empirical relationship between the stress and velocity gradients, it has been successfully applied to non-Newtonian fluids experimentally. The two constants in the model can be chosen with great ease for specific fluids and the

* Corresponding author. Tel.: +1 407 823 5089; fax: +1 407 823 6253.
E-mail address: vajravel@pegasus.cc.ucf.edu (K. Vajravelu).

0017-9310/$ - see front matter © 2009 Elsevier Ltd. All rights reserved.
doi:10.1016/j.ijheatmasstransfer.2009.05.022

Nomenclature

A, D	constants
b	stretching rate, a positive constant
B_0	magnetic field
C_f	skin friction
C_p	specific heat at constant pressure
D_{ij}	strain tensor
Ec	modified Eckert number
f	dimensionless velocity
$h(x)$	heat transfer coefficient
j	Joule effect
K	consistency coefficient
K^*	mean absorption coefficient
l	characteristic length
M	hypergeometric (Kummer's) function
Mn	magnetic parameter
n	power law index
Nu_x	Nusselt number
Nr	thermal radiation parameter
p	pressure
Pr	modified Prandtl number
Q	internal heat generation/absorption
q_w	local heat flux at the sheet
q_r	radiative heat flux
R	surface mass transfer
Re_x	local Reynolds number
T	temperature distribution
T_{ij}	stress tensor
T_w	temperature at the sheet
T_∞	temperature of the fluid at infinity
u	velocity in the x-direction
$U = bx$	velocity of the sheet
v	velocity in the y-direction
x	horizontal distance
y	vertical distance

Greek symbols

$\alpha(T)$	thermal conductivity
α_∞	thermal conductivity at infinity
β	heat source/sink parameter
γ	kinematic viscosity of the power law fluid
δ_{ij}	Kronecker delta
ρ	density
μ^*	consistency index of the power law fluid
ψ	stream function
η	similarity variable
ε	small parameter
θ	dimensionless temperature distribution
σ	electrical conductivity
σ^*	Stephan–Boltzmann constant
$\Delta T = T_w - T_\infty$	sheet temperature
τ	shear stress

Subscripts

w, ∞	conditions at the surface and in the free stream
η	differentiation with respect to η

model is found to be good in representing pseudo-plastic behavior. It is frequently used in oil engineering. A considerable amount of work has been done in this field by taking into account the heat and mass transfer. Schowalter [17] has introduced the concept of boundary layer theory of non-Newtonian fluids. Acrivos et al. [18] have investigated the steady laminar flow of non-Newtonian fluids over a plate. Lee and Ames [19] extended the above work to find the similarity solutions for non-Newtonian power law fluid. Andersson et al. [20] studied the boundary layer flow of an electrically conducting incompressible fluid obeying the power law model in the presence of transverse magnetic field. Howell et al. [21] examined the momentum and heat transfer occurring in the laminar boundary layer on a continuously moving and stretching surface in a non-Newtonian power law fluid. Mahmoud and Mahmoud [22] investigated the problem of a two-dimensional steady incompressible power law non-Newtonian electrically conducting fluid past a continuously moving surface in the presence of a transverse magnetic field. However all these studies are restricted to the analyses of either flow characteristics or flow and heat transfer characteristics over an impervious stretching boundary. We know that the characteristic properties of the final product of the material depend to a great extent on the rate of cooling through the adjacent boundary. The rate of cooling associated with the heat transfer phenomena may be controlled by suction/blowing through the porous boundary in the presence of a constant transverse magnetic field. Hassanien et al. [23] presented a work on flow and heat transfer in power law fluid over a stretching porous surface with variable surface temperature. Very recently, Abel and Mahesha [24] considered the effects of buoyancy and variable thermal conductivity in a power law fluid past a vertical stretching sheet in the presence of non-uniform heat source.

All the above investigators restrict their analyses to MHD flow and heat transfer over a stretching sheet. However the intricate flow and heat transfer problem with the effects of internal heat generation/absorption, viscous dissipation, work done by stress, and the thermal radiation is yet to be studied. This has applications to several industrial problems (say engineering processes involving nuclear power plants, gas turbines, and many others, see Vajravelu [25], Vajravelu and Nayfeh [26]). In all these studies, the thermo-physical properties of the ambient fluids were assumed to be constant. However it is well known that these properties may change with temperature, especially the thermal conductivity. Available literature on variable thermal conductivity [27–31] shows that this type of flow has not been investigated for power law fluids in the presence of suction/bowing and impermeability of the stretching sheet.

In view of these applications, we study the flow and heat transfer phenomena in a power law fluid over a porous stretching surface, in the presence of uniform transverse magnetic field, taking into account the internal heat generation/absorption, viscous dissipation, work done by stress, variable thermal conductivity, and thermal radiation. This is a generalization of Andersson et al.'s [20] work to the case of power law fluid flow and heat transfer where the thermal conductivity is a function of temperature in the presence of transverse magnetic field. Recently, flow of non-Newtonian polymer solution was investigated by Savvas et al. [32] and it was shown that computer simulation is a powerful technique to predict the flow behavior. Because of the complexity and non-linearity of our problem, the resulting equations are solved numerically by the Keller–Box method. One of the important observations of the study is that suction reduces the horizontal velocity where as blowing increases the horizontal velocity for all values of power law index.

2. Flow analysis

Consider a viscous, steady two-dimensional flow of an incompressible, electrically conducting power law fluid in the presence of a transverse magnetic field over a stretching sheet lying on the

plane $y > 0$. The flow is confined to $y > 0$ (for details, see [20]). The flow is generated by stretching the sheet from the origin with the application of two equal and opposite forces in such a way that the velocity of the sheet is linear. The thermo-physical properties of the sheet and the fluid are assumed to be constant except for the viscosity of the power law fluid which depends on the shear rate. The flow is subject to a transverse uniform magnetic field of strength $\vec{B}_0 = (0, B_0, 0)$. Application of such a magnetic field stabilizes the boundary layer flow. The magnetic Reynolds number is considered to be small so that the induced magnetic field is negligible. We also take the strength of the electric field due to polarization of the electric charges to be negligibly small. Under these assumptions, the governing boundary layer equations of motion are

$$\frac{\partial u}{\partial x} + \frac{\partial v}{\partial y} = 0, \tag{1}$$

$$u\frac{\partial u}{\partial x} + v\frac{\partial v}{\partial y} = \frac{1}{\rho}\frac{\partial T_{xy}}{\partial y} - \frac{\sigma B_0^2}{\rho}u, \tag{2}$$

where u and v are the velocity components in the stream-wise and the cross section directions, respectively; and ρ, σ, and B_0 are the density, electric conductivity, and magnetic field, respectively. The power law fluid represented by the rheological equation of state is given by

$$T_{ij} = -p\delta_{ij} + 2K(D_{kl}D_{kl})^{\frac{n-1}{2}}D_{ij}, \tag{3}$$

where T_{ij} and D_{ij} are, respectively, the stress and strain rate tensors, K is the consistency coefficient, n is the power law index. The two parameter rheological equation (3) is known as the Ostwald–de-Waele model equation or more commonly called the power law model. When $n = 1$, Eq. (3) represents a Newtonian fluid with dynamic coefficient of viscosity K. For $n \neq 1$, the constitutive equation (3) represents the shear thinning ($n < 1$) and the shear thickening ($n > 1$) fluids. Due to the boundary layer approximation, the essential off-diagonal stress component can be written as

$$T_{xy} = K\left(\frac{\partial u}{\partial y}\frac{\partial u}{\partial y}\right)^{\frac{n-1}{2}}\frac{\partial u}{\partial y} = -K\left(-\frac{\partial u}{\partial y}\right)^{n}, \tag{4}$$

and this is the only stress component of dynamic significance. Now the governing momentum equation (2) reduces to the following form:

$$u\frac{\partial u}{\partial x} + v\frac{\partial v}{\partial y} = -\frac{K}{\rho}\frac{\partial}{\partial y}\left(-\frac{\partial u}{\partial y}\right)^{n} - \frac{\sigma B_0^2}{\rho}u. \tag{5}$$

However, unlike the second-order visco-elastic fluid, the inelastic power law model (3) does not exhibit normal stress differences. In the present situation, we have $\frac{\partial u}{\partial y} \leq 0$ throughout the boundary layer since the stream-wise velocity component u decreases monotonically with the distance y from the moving surface. The appropriate boundary conditions for the present flow problem are

$$u(x, 0) = U, \tag{6a}$$

$$v(x, 0) = v_w, \tag{6b}$$

$$u \to 0 \quad \text{as} \quad y \to \infty, \tag{6c}$$

where v_w is the suction velocity across the stretching sheet when $v_w < 0$, and it is blowing velocity when $v_w > 0$. To examine the flow adjacent to the plate, the following transformations are used:

$$\eta = \frac{y}{x}(Re_x)^{\frac{1}{n+1}}, \quad \psi(x, y) = bx^2(Re_x)^{\frac{-1}{n+1}}f(\eta), \tag{7}$$

where η is the similarity variable and $\psi(x, y)$ is the stream function. The velocity components u and v are given by

$$(u, v) = \left(\frac{\partial \psi}{\partial y}, -\frac{\partial \psi}{\partial x}\right). \tag{8}$$

The local Reynolds number is defined as

$$Re_x = \frac{U^{2-n}x^n}{\gamma}. \tag{9}$$

The conservation of mass equation (1) is therefore automatically satisfied. The momentum equation (5) and the boundary conditions (6) can be written as

$$n(-f_{\eta\eta})^{n-1}f_{\eta\eta\eta} - f_\eta^2 + \left(\frac{2n}{n+1}\right)ff_{\eta\eta} - Mnf_\eta = 0, \tag{10}$$

$$f_\eta(0) = 1, \tag{11a}$$

$$f(0) = R, \tag{11b}$$

$$f_\eta(\eta) \to 0 \quad \text{as} \quad \eta \to \infty. \tag{11c}$$

Here the subscript η denotes differentiation with respect to η and $Mn = \frac{\sigma B_0^2}{\rho b}$ is the magnetic parameter. It should be noted that the velocity $U = U(x)$ is used to define the dimensionless stream function f in Eq. (7). The local Reynolds number in Eq. (9) is the velocity of the moving surface that drives the flow. This choice is in contrast with the conventional boundary layer analysis in which the free stream velocity is taken as the velocity scale. Although the transformation defined in (7) can be used for an arbitrary variation of $U(x)$, the transformation results in a true similarity problem only if U varies as Cx^m ($m = 1$). Here m is an arbitrary positive constant (not necessarily an integer). In the conditions (11) the horizontal injection or suction speed v_w must be a function of the distance ($m \neq 1$) from the leading edge. Consequently v_w can be rewritten as

$$R = -\frac{n+1}{2n}\left(\frac{(Re_x)^{1/n+1}}{U}\right)v_w. \tag{12}$$

In order to have a similarity solution in η, it should be noted that v_w must be of the order of magnitude of $u_w(Re_x)^{-\frac{1}{n+1}}$, for $n \neq 1$. This is to ensure that flow with suction or blowing at the surface satisfies the boundary layer assumptions. Therefore, R is introduced to represent the surface mass transfer which is positive for blowing, negative for suction, and of order one. Eq. (12) shows that, the suction or blowing parameter R is used to control the strength and direction of the normal flow at the boundary. Three boundary conditions in (11) are sufficient for solving the third-order equation in (10). This contrasts with boundary layer flow of a visco-elastic fluid, for which the resulting fourth-order equation requires an extra boundary condition for solvability. This issue has been discussed in detail by Rajagopal et al. [33]. The skin friction coefficient at the sheet is given by

$$C_f = \frac{-2T_{xy}(0)}{\rho U^2} = 2(Re_x)^{\frac{-1}{n+1}}[-f_{\eta\eta}(0)]^n. \tag{13}$$

To determine the temperature distribution and rate of heat transfer in the above boundary layer, we now solve the energy equation related to the stretching sheet problem.

3. Heat transfer analysis

The energy equation for a fluid with variable thermal conductivity in the presence of internal heat generation/absorption, viscous dissipation, work done by stress, and thermal radiation for the above two-dimensional flow is

$$\rho c_p\left(u\frac{\partial T}{\partial x} + v\frac{\partial T}{\partial y}\right) = \frac{\partial}{\partial y}\left(\alpha(T)\frac{\partial T}{\partial y}\right) + Q(T - T_\infty) + \mu\left(\frac{\partial u}{\partial y}\right)^{n+1} + \sigma B_0^2 u^2 - \frac{\partial q_r}{\partial y}, \tag{14}$$

subject to the appropriate boundary conditions. In the above equation, c_p is the specific heat at constant pressure, T is the temperature

of the fluid, T_∞ is the free stream temperature, and $\alpha(T)$ is the temperature-dependent thermal conductivity. We consider the temperature-dependent thermal conductivity in the following form (Chiam [27]):

$$\alpha(T) = \alpha_\infty\left(1 + \varepsilon\frac{T - T_\infty}{\Delta T}\right), \tag{15}$$

where ε is a small parameter, $\Delta T = T_w - T_\infty$, T_w is the given temperature at the wall, and α_∞ is the thermal conductivity of the fluid far away from the sheet. The term containing Q represents the temperature-dependent heat source when $Q > 0$ and heat sink when $Q < 0$; and it deals, respectively, with the situations of exothermic and endothermic chemical reactions. The third and fourth terms on the right-hand side of Eq. (14) represent, respectively, the viscous dissipation and the ohmic heating effect. The last term q_r on the right-hand side of Eq. (14) represents the radiative heat flux which is given by

$$q_r = -\frac{4\sigma^*}{3K^*}\frac{\partial T^4}{\partial y}, \tag{16}$$

where σ^* *and* K^* are, respectively, the Stephan–Boltzmann constant and the mean absorption coefficient. We assume that the differences within the flow are such that T^4 may be expressed as a linear function of temperature. This is accomplished by expanding T^4 in a Taylor series about T_∞ and neglecting the higher order terms to obtain $T^4 \cong 4T_\infty^3 T - 3T_\infty^4$. Using this expression of T^4 in Eq. (16), we get

$$q_r = -\frac{16}{3}\frac{\sigma^*}{K^*}T_\infty^3\frac{\partial T}{\partial y}. \tag{17}$$

Substituting (15)–(17) in (14) we get

$$\begin{aligned}&\rho c_p u\frac{\partial T}{\partial x} + \left(\rho c_p v - \frac{\alpha_\infty\varepsilon}{\Delta T}\frac{\partial T}{\partial y}\right)\frac{\partial T}{\partial y}\\ &= \alpha_\infty\left(1 + \frac{\varepsilon}{\Delta T}(T - T_\infty) + \frac{16\sigma^* T_\infty^3}{3K^*\alpha_\infty}\right)\frac{\partial^2 T}{\partial y^2}\\ &\quad + \mu\left(\frac{\partial u}{\partial y}\right)^{n-1}\left(\frac{\partial u}{\partial y}\right)^2 + \sigma B_0^2 u^2 + Q(T - T_\infty)\end{aligned} \tag{18}$$

From Eq. (18) it is observed that the effect of ε and thermal radiation is to enhance the thermal diffusivity.

The appropriate boundary conditions are

$$\begin{aligned}&T = T_w = T_\infty + A\left(\frac{x}{l}\right)^2 \quad \text{at} \quad y = 0,\\ &T \to T_\infty \quad \text{as} \quad y \to \infty,\end{aligned} \tag{19}$$

where A is a constant, which depends on the properties of the fluid and l is a characteristic length. In practice, when computing numerical solutions, the last condition is imposed at sufficiently large distance from the sheet. This distance depends on the physical parameters and can be determined by carefully performed numerical experiments. In terms of the dimensionless temperature,

$$\theta = \frac{T - T_\infty}{T_w - T_\infty}, \quad \text{where} \quad T_w - T_\infty = A\left(\frac{x}{l}\right)^2. \tag{20}$$

The energy equation (18) reduces to the following non-linear ordinary differential equation:

$$\begin{aligned}&(K_0 + \varepsilon\theta)\theta_{\eta\eta} + \varepsilon\theta_\eta^2 + Pr\left(\frac{2n}{n+1}f\theta_\eta - (2f_\eta - \beta)\theta\right)\\ &= -Pr\,Ec\left\{(f_{\eta\eta})^{n+1} + Mnf_\eta^2\right\},\end{aligned} \tag{21}$$

subject to the boundary conditions

$$\theta(\eta) = 1 \quad \text{at} \quad \eta = 0, \quad \theta(\eta) \to 0 \quad \text{as} \quad \eta \to \infty. \tag{22}$$

Here again, the subscript η denotes the differentiation with respect to η. The parameters Pr, β, Ec, and Nr are the modified Prandtl number, heat source/sink parameter, modified Eckert number and the thermal radiation parameter, respectively, and are defined by

$$\begin{aligned}&Pr = \frac{\rho c_p b x^2}{\alpha_\infty}(Re_x)^{\frac{-2}{n+1}}, \quad \beta = \frac{Q}{\rho c_p b}, \quad Ec = \frac{\gamma l^2 b^n}{c_p A x^2}Re_x,\\ &Nr = \frac{K^*\alpha_\infty}{4\sigma^* T_\infty^3}, \quad K_0 = \frac{3Nr}{3Nr + 4}.\end{aligned} \tag{23}$$

The local Nusselt number is given by

$$Nu_x = \frac{h(x)}{\alpha_\infty}, \tag{24}$$

where the heat transfer coefficient $h(x)$ has the form

$$h(x) = \frac{q_w(x)}{T_w - T_\infty}, \tag{25}$$

and the local heat flux at the sheet is

$$q_w = -\alpha_\infty\left(\frac{\partial T}{\partial y}\right)_{y=0} = -\alpha_\infty\left(\frac{U^{2-n}}{\gamma x}\right)^{\frac{1}{n+1}}\theta_\eta(0). \tag{26}$$

4. Numerical procedure

The momentum and the energy equations for the non-Newtonian power law fluid over a stretching sheet in the presence of a transverse magnetic field is presented in this paper. The effects of the porous boundary, viscous dissipation, ohmic dissipation, temperature-dependent thermal conductivity, heat source/sink, and radiation are taken into consideration. The boundary layer partial differential equations are transformed into a system of non-linear coupled ordinary differential equations. The transformed equations (10) and (21), together with the boundary conditions (11) and (22) are solved numerically using the Keller–Box method (Prasad et al. [34]). The computed numerical values are plotted graphically in Figs. 1–11 and presented in Tables 1 and 2. To assess the accuracy of the computed results, the values of the skin friction are compared with the values obtained by Andersson et al. [20], for the case of impermeability of the stretching sheet ($V_w = 0$). It is observed that our results are in good agreement with the results of Andersson et al. [20] as seen from the tabulated results in

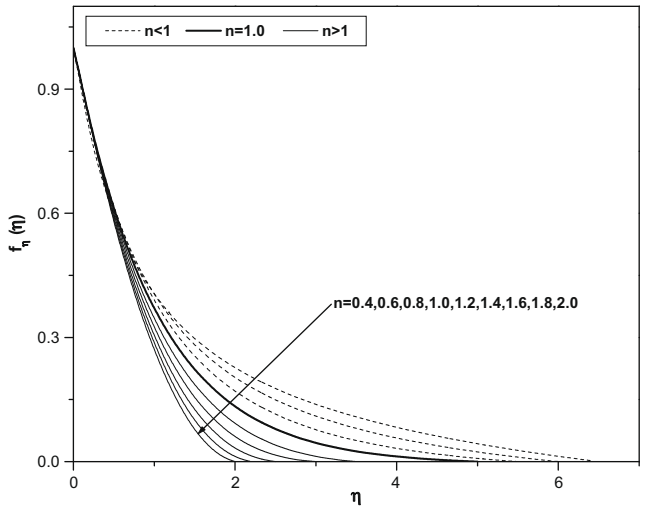

Fig. 1. Horizontal velocity profiles $f_\eta(\eta)$ vs. η for different values of n with $Mn = 0.0$, $V_w = 0.0$.

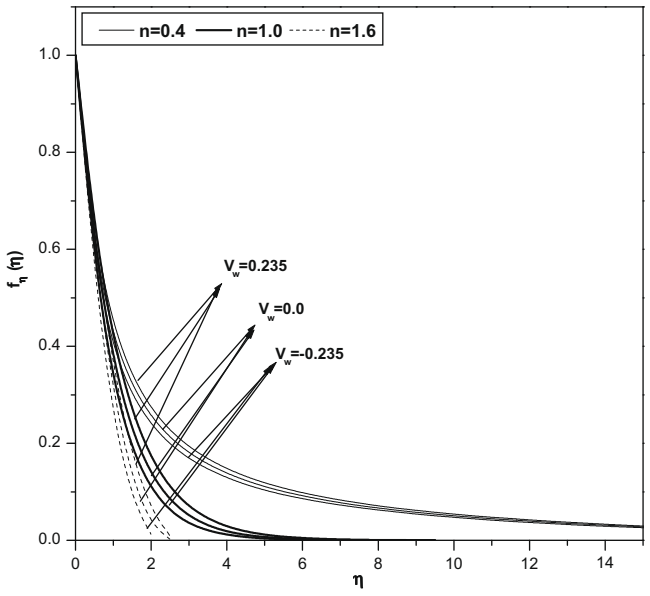

Fig. 2. Horizontal velocity profiles $f_\eta(\eta)$ vs. η for different values of power law index n and V_w with $Mn = 0.0$.

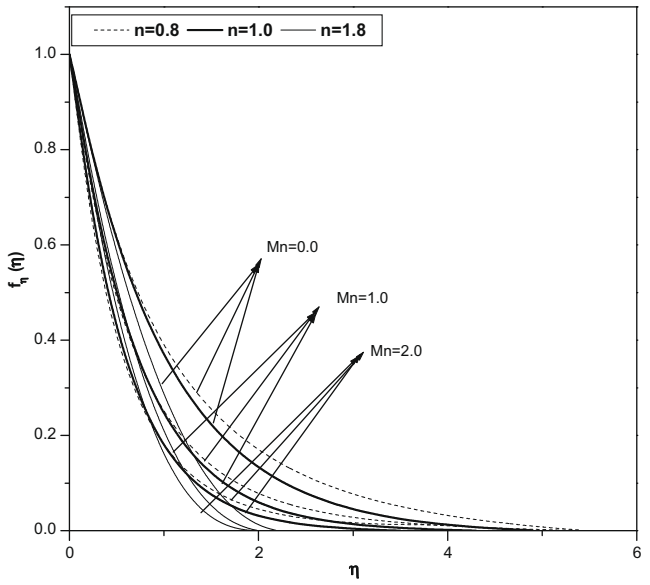

Fig. 4. Horizontal velocity profiles $f_\eta(\eta)$ vs. η for different values of Mn and power law index n with $V_w = 0.0$.

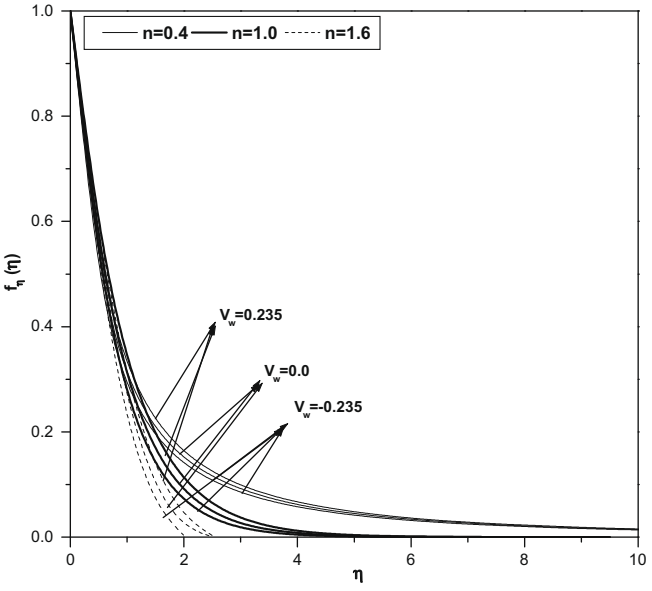

Fig. 3. Horizontal velocity profiles $f_\eta(\eta)$ vs. η for different values of power law index n and V_w with $Mn = 0.5$.

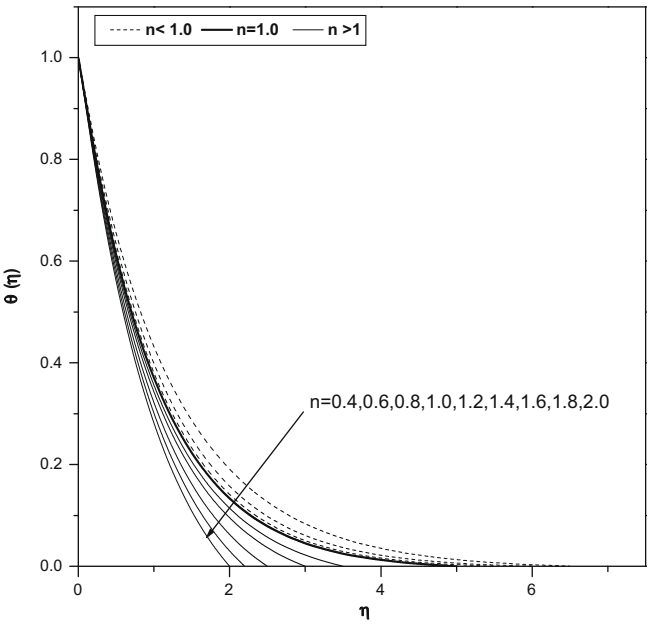

Fig. 5. Temperature profiles $\theta(\eta)$ vs. η for different values of n with $Mn = 0.0$, $\beta = 0.0$, $Pr = 1.0$, $\varepsilon = 0.0$, $Nr = 1000.0$.

Table 1. Numerical results for horizontal velocity and the temperature are, respectively, shown in Figs. 1–11. Table 2 provides the numerical results for the skin friction for different values of n, Mn and V_w. Table 3 provides the numerical results for the wall temperature gradient (Nusselt number) for different values of the physical parameters.

5. Discussion of the results

Figs. 1–4 illustrate the effects of the power law index n, the magnetic parameter Mn, the suction, and the impermeability parameter on the horizontal velocity $f_\eta(\eta)$. It can be seen that the horizontal velocity is monotonically tends to zero as the distance increases from the boundary. The effect of the increasing values of the power law index n is to reduce the horizontal boundary layer thickness. That is, the thickness is much larger for shear thinning (pseudo plastic; $0 < n < 1$) fluids than that of shear thickening (dilatants; $1 < n < 2$) fluids. This behavior is noticeable in Fig. 1. The effect of the impermeability of the boundary wall suction on the horizontal velocity in the absence of magnetic parameter Mn is shown in Fig. 2. It can be seen that the suction reduces the horizontal boundary layer thickness whereas the blowing has the opposite effect on the horizontal velocity boundary layer. These results are consistent with the physical situation. In Fig. 3 the horizontal velocity profiles are presented for the same set of physical parameters except for non-zero values of magnetic parameter Mn. Com-

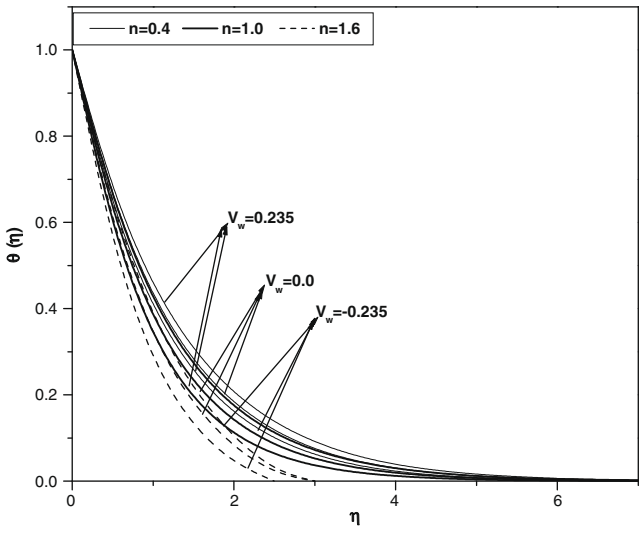

Fig. 6. Temperature profiles $\theta(\eta)$ vs. η for different values of power law index (n) and $Mn = 0.0$, $V_w = 0.0$.

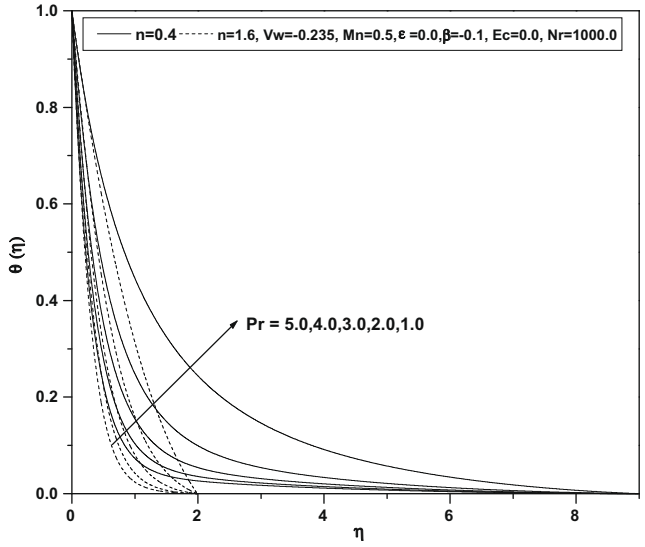

Fig. 8. Temperature profiles $\theta(\eta)$ vs. η for different values of Prandtl number.

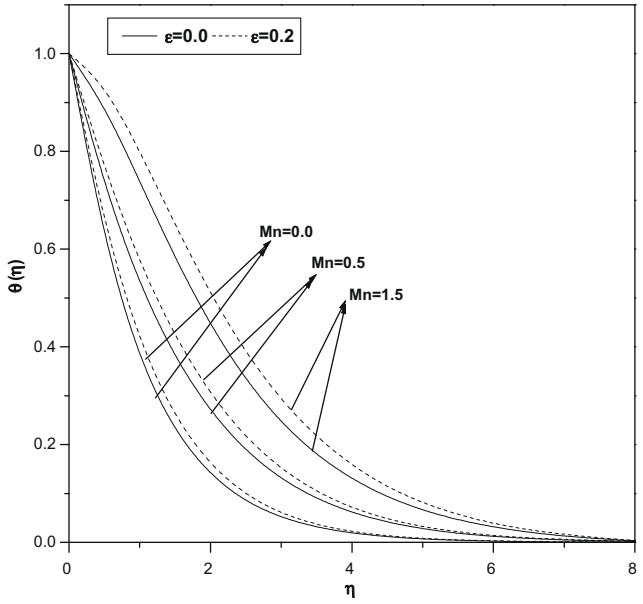

Fig. 7. Variation of temperature profiles $\theta(\eta)$ vs. η for different values of *Mn and* ε (with $n = 1.0$, $V_w = 0.0$).

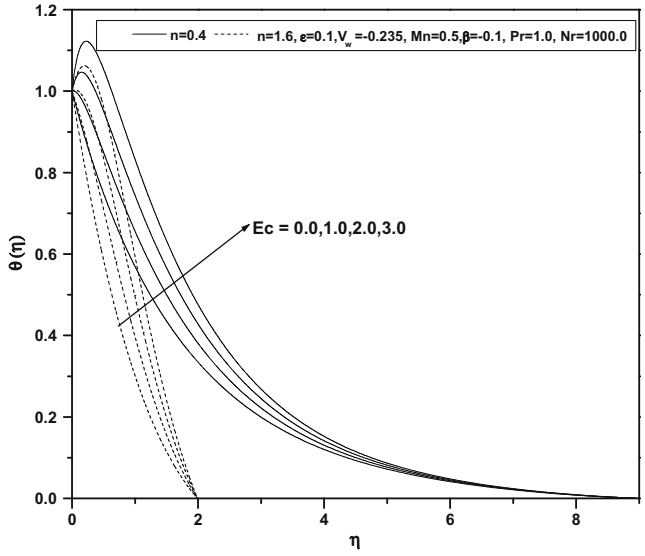

Fig. 9. Temperature profiles $\theta(\eta)$ vs. η for different values of Eckert number.

parison of these two figures reveals that the effect of magnetic parameter (Mn) is to decrease the velocity for the cases of suction. This is due to the fact that, the introduction of a transverse magnetic field, normal to the flow direction, has a tendency to create the drag known as the Lorentz force which tends to resist the flow. Hence the horizontal velocity profiles decrease as the magnetic parameter Mn increases. This behavior is true in the cases of shear thinning and shear thickening fluids. This behavior is very much in evidence in the case of an impermeable boundary wall (see Fig. 4).

The effects of the power law index n, the magnetic parameter Mn, the Prandtl number Pr, the Eckert number Ec, the thermal radiation parameter Nr and the heat source parameter β on temperature are shown in Figs. 5–11 in the presence of suction. It is observed from these figures that the temperature distribution $\theta(\eta)$ asymptotically tends to zero in the free stream region. The effect of the power law index n on the temperature distribution $\theta(\eta)$ in the boundary layer is shown in Fig. 5. Increasing the values of the power law index leads to thinning of the thermal boundary layer thickness. This behavior holds for shear thinning and shear thickening fluids.

Fig. 6 depicts the effects of the suction parameter on the temperature distribution. The thermal boundary layer becomes thicker for suction and thinner for blowing. The effects of the magnetic parameter Mn and the variable thermal conductivity parameter ε on the temperature distribution $\theta(\eta)$ are depicted in Fig. 7. The effect of the magnetic parameter Mn is to increase the temperature profile and it tends to zero as the distance increases from the boundary. As explained above, the transverse magnetic field gives rise to a resistive force known as the Lorentz force of an electrically conducting fluid. This force makes the fluid experience a resistance by increasing the friction between its layers and thus increases its temperature. This behavior holds even in the presence of variable

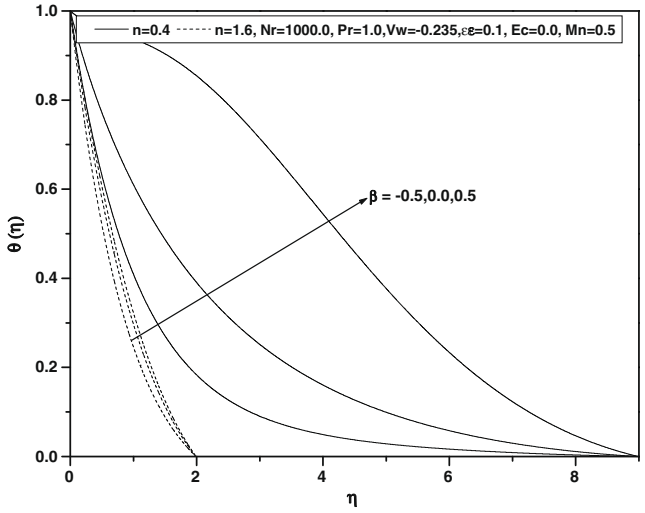

Fig. 10. Temperature profiles $\theta(\eta)$ vs. η for different values of heat source/sink parameter.

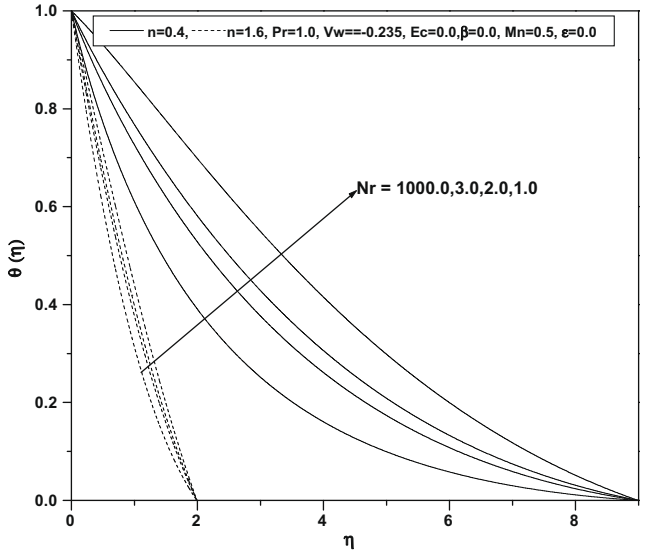

Fig. 11. Temperature profiles $\theta(\eta)$ vs. η for different values of thermal radiation parameter.

thermal conductivity parameter. This is due to the fact that the presence of temperature-dependent thermal conductivity results in a reduction in the magnitude of the transverse velocity by a quantity $\frac{\partial k(T)}{\partial y}$, and this can be seen from energy equation. This behavior holds for shear thinning and shear thickening fluids. The effect of Prandtl number on the temperature distribution is shown in Fig. 8. From the graphical representation we notice that the effect of an increase in the Prandtl number is to decrease the temperature distribution. This is due to the fact that thermal boundary layer thickness decreases with the increase of Prandtl number. From Figs. 7 and 8, we notice that the effect of negative values of V_w (suction) is to decrease the temperature throughout the flow field.

The graphs for the temperature distribution for different values of the Eckert number are plotted in Fig. 9. From this figure we see that the effect of increasing Eckert number is to increase the temperature distribution $\theta(\eta)$. This is in conformity with the fact that

Table 1
Comparison of skin friction – $f''(0)$ values with Andersson et al. [20].

	$n = 0.4$	$n = 0.6$	$n = 0.8$	$n = 1.0$	$n = 1.2$	$n = 1.5$	$n = 2.0$
Andersson et al. [20]	1.273	1.096	1.029	1.00	0.987	0.981	0.980
Present study	1.27968	1.09838	1.02897	1.00000	0.98738	0.98058	0.98035

Table 2
Values of skin friction – $f_{\eta\eta}(0)$ for different values of Mn and n.

N	Mn	Skin friction – $f_{\eta\eta}(0)$		
		$V_w = -0.235$	$V_w = 0.0$	$V_w = 0.235$
0.4	0.0	1.44505417	1.29193401	1.16056228
	0.5	2.01030493	1.8151418	1.64491689
0.8	0.0	1.15884542	1.03153598	0.91997683
	0.5	1.44237614	1.30816805	1.18788457
1.0	0.0	1.12457597	1.00029111	0.889754415
	0.5	1.34787822	1.22475886	1.11288595
1.2	0.0	1.10885763	0.987372041	0.877078414
	0.5	1.29024136	1.17498946	1.06866932
1.6	0.0	1.09335208	0.979825199	0.871911228
	0.5	1.22387087	1.12067473	1.02223969
2.0	0.0	1.08608031	0.980356693	0.874927878
	0.5	–	1.09269071	1.00212872

energy is stored in the fluid region as a consequence of dissipation due to viscosity and elastic deformation. In Fig. 10 the temperature distribution for different values of the heat source parameter are drawn. The direction of heat flow depends both on temperature difference $(T_w - T_\infty)$ and the temperature gradient $\theta_\eta(0)$. To interpret the heat transfer result physically, we discuss the result of positive β and the negative β separately. For positive β we have a heat source in the boundary layer when $T_w < T_\infty$ and a heat sink when $T_w < T_\infty$. Physically these correspond, respectively, recombination and dissociation within the boundary layer. For the case of a cooled wall $(T_w < T_\infty)$, there is heat transfer from the fluid to the wall even without heat source. The presence of a heat source $\beta > 0$ will further increase the heat flow to the wall. When β is negative, this indicates a heat source for $(T_w > T_\infty)$ and a heat sink $(T_w < T_\infty)$. This corresponds to combustion and an endothermic chemical reaction. For the case of heated wall $(T_w > T_\infty)$, the presence of a heat source creates a layer of hot fluid adjacent to the surface and therefore heat at the wall decreases. For the cooled wall case $(T_w < T_\infty)$, the presence of a heat sink blankets the surface with a layer of cool fluid, and hence the heat flow at the surface decreases. This result is similar to the result obtained by Acharya et al. [35].

The effect of thermal radiation on the temperature distribution $\theta(\eta)$ for shear thinning and shear thickening fluids is shown in Fig. 11. The effect of increasing values of thermal radiation is to decrease the temperature distribution in the flow region. It is observed that the increase in thermal radiation produces a significant decrease in the thickness of the thermal boundary layer of the fluid, and so the temperature profile decreases in the case of shear thickening and shear thinning fluids. The values of skin friction and Nusselt number for various values of the non-dimensional parameters are recorded in Tables 2 and 3, respectively. It is found that the skin friction coefficient increases as the power law index increases whereas it decreases as the magnetic parameter increases. The effect of the Prandtl number is to reduce the wall temperature gradient for the cases of suction and impermeability of the sheet.

Table 3
Wall temperature gradient $\theta_\eta(0)$ for different values of the physical parameters.

n	Nr	Ec	β	ε	$Mn = 0.0$						$Mn = 0.5$					
					$V_w = -0.235$		$V_w = 0.0$		$V_w = 0.235$		$V_w = -0.235$		$V_w = 0.0$		$V_w = 0.235$	
					$Pr = 1.0$	$Pr = 2.0$	$Pr = 1.0$	$Pr = 2.0$	$Pr = 1.0$	$Pr = 2.0$	$Pr = 1.0$	$Pr = 2.0$	$Pr = 1.0$	$Pr = 2.0$	$Pr = 1.0$	$Pr = 2.0$
0.4	10,000	0	0	0	−1.2092	−1.7574	−1.2613	−1.8757	−1.316	−2.0028	−0.8491	−1.452	−0.8943	−1.5572	−0.945	−1.6741
				0.1	−1.1604	−1.6957	−1.2116	−1.8133	−1.2657	−1.9402	−0.7613	−1.3623	−0.804	−1.4647	−0.8537	−1.58025
				0.2	−1.1074	−1.6305	−1.1575	−1.7474	−1.2109	−1.8741	−0.6185	−1.2364	−0.663	−1.3421	−0.7179	−1.46075
			0.05	0	−1.1695	−1.7012	−1.2184	−1.8129	−1.2698	−1.9328	−0.813	−1.3997	−0.8557	−1.4991	−0.9038	−1.60973
				0.1	−1.122	−1.6412	−1.1701	−1.7523	−1.2208	−1.872	−0.7264	−1.312	−0.7669	−1.4088	−0.8141	−1.51817
				0.2	−1.0704	−1.578	−1.1174	−1.6883	−1.1675	−1.8078	−0.5837	−1.1878	−0.6265	−1.2885	−0.6794	−1.40128
		1	0	0	−0.9133	−1.499	−0.9193	−1.571	−0.9209	−1.6442	−0.347	−1.0033	−0.3254	−1.0396	−0.3008	−1.07876
				0.1	−0.8599	−1.4331	−0.8646	−1.5038	−0.865	−1.5762	−0.2505	−0.9059	−0.2258	−0.9386	−0.1998	−0.97576
				0.2	−0.8015	−1.3632	−0.8045	−1.4324	−0.8036	−1.5039	−0.094	−0.7698	−0.0708	−0.8053	−0.0502	−0.84516
			0.05	0	−0.8747	−1.4442	−0.8779	−1.5103	−0.8766	−1.577	−0.3097	−0.9514	−0.286	−0.9826	−0.259	−1.01611
				0.1	−0.8226	−1.3801	−0.8245	−1.4448	−0.822	−1.5107	−0.2138	−0.8555	−0.1872	−0.8833	−0.1591	−0.91506
				0.2	−0.7655	−1.312	−0.7658	−1.3753	−0.762	−1.4403	−0.0558	−0.7203	−0.0314	−0.7517	−0.0093	−0.78652
	1	0	0	0	−0.7431	−1.1096	−0.7587	−1.1523	−0.7747	−1.1971	−0.3236	−0.7374	−0.3417	−0.7748	−0.3622	−0.81702
				0.1	−0.7039	−1.063	−0.7183	−1.1048	−0.7333	−1.1488	−0.2455	−0.6501	−0.2615	−0.6851	−0.2808	−0.72624
				0.2	−0.6573	−1.0118	−0.67	−1.0524	−0.6835	−1.0956	−0.1343	−0.5091	−0.147	−0.5438	−0.1646	−0.58859
			0.05	0	−0.732	−1.0935	−0.747	−1.135	−0.7625	−1.1786	−0.3136	−0.7228	−0.3314	−0.7594	−0.3516	−0.80064
				0.1	−0.6932	−1.0474	−0.7071	−1.0881	−0.7215	−1.1309	−0.2358	−0.636	−0.2516	−0.6702	−0.2707	−0.71049
				0.2	−0.6471	−0.9968	−0.6593	−1.0363	−0.6723	−1.0783	−0.1248	−0.4951	−0.1374	−0.5291	−0.1549	−0.57326
		1	0	0	−0.4074	−0.8058	−0.3774	−0.8026	−0.341	−0.7944	0.2305	−0.2247	0.2771	−0.1957	0.32951	−0.1631
				0.1	−0.3633	−0.7546	−0.3317	−0.75	−0.2939	−0.7405	0.3172	−0.1285	0.3663	−0.0965	0.4203	−0.06248
				0.2	−0.3102	−0.6978	−0.2765	−0.6915	−0.2367	−0.6806	0.4405	0.0265	0.4936	0.05912	0.54972	0.08947
			0.05	0	−0.3966	−0.7902	−0.3661	−0.786	−0.3292	−0.7766	0.242	−0.2094	0.2888	−0.1797	0.34148	−0.14631
				0.1	−0.3528	−0.7395	−0.3208	−0.7339	−0.2825	−0.7233	0.3287	−0.1134	0.378	−0.0808	0.4322	−0.04603
				0.2	−0.3002	−0.6832	−0.266	−0.6759	−0.2257	−0.664	0.4523	0.0422	0.5055	0.07527	0.56178	0.10612
1.0	10,000	0	0	−0.1	−1.2793	−1.8338	−1.3799	−2.0553	−1.4901	−2.3033	−0.9825	−1.5905	−1.0835	−1.804	−1.1992	−2.04998
				0	−1.2347	−1.7785	−1.3343	−1.9998	−1.4442	−2.2485	−0.921	−1.5229	−1.0219	−1.7364	−1.139	−1.98395
				0.05	−1.2111	−1.75	−1.3103	−1.9711	−1.4201	−2.2203	−0.8867	−1.4869	−0.9878	−1.7006	−1.1061	−1.94933
			0.05	−0.1	−1.2379	−1.777	−1.3328	−1.9865	−1.4366	−2.2212	−0.9438	−1.5364	−1.0396	−1.7389	−1.1496	−1.97217
				0	−1.1945	−1.7233	−1.2884	−1.9326	−1.3919	−2.1679	−0.8835	−1.4705	−0.9793	−1.673	−1.0906	−1.90787
				0.05	−1.1716	−1.6956	−1.265	−1.9048	−1.3684	−2.1405	−0.8497	−1.4354	−0.9458	−1.6381	−1.0583	−1.87414
		1	0	−0.1	−1.0101	−1.613	−1.0501	−1.7748	−1.0906	−1.9529	−0.6101	−1.2782	−0.6452	−1.4245	−0.6883	−1.59538
				0	−0.96	−1.5531	−0.998	−1.7136	−1.0374	−1.8914	−0.5408	−1.2041	−0.5749	−1.3493	−0.6187	−1.52093
				0.05	−0.9334	−1.5221	−0.9704	−1.6819	−1.0091	−1.8596	−0.502	−1.1646	−0.5359	−1.3094	−0.5805	−1.48173
			0.05	−0.1	−0.9703	−1.5578	−1.0052	−1.7089	−1.0403	−1.8751	−0.5708	−1.2248	−0.6016	−1.3614	−0.6397	−1.52111
1.6	10,000	1		0	−0.9212	−1.4995	−0.9543	−1.6493	−0.9881	−1.8152	−0.5024	−1.1522	−0.5322	−1.2878	−0.5711	−1.4483
				0.05	−0.8952	−1.4692	−0.9272	−1.6184	−0.9605	−1.7841	−0.4638	−1.1134	−0.4935	−1.2486	−0.5333	−1.40993
	1	0	0	−0.1	−0.7894	−1.1758	−0.8207	−1.259	−0.8546	−1.3498	−0.4379	−0.8676	−0.4808	−0.9531	−0.5297	−1.05125
				0	−0.7532	−1.1329	−0.7828	−1.2149	−0.8154	−1.3052	−0.3848	−0.8071	−0.427	−0.8924	−0.4761	−0.9917
				0.05	−0.7336	−1.1101	−0.7622	−1.1915	−0.7941	−1.2815	−0.355	−0.7731	−0.3968	−0.8585	−0.4461	−0.95884
			0.05	−0.1	−0.7776	−1.159	−0.8079	−1.24	−0.8408	−1.3284	−0.427	−0.8519	−0.4691	−0.9355	−0.5171	−1.0315
				0	−0.7418	−1.1165	−0.7705	−1.1964	−0.802	−1.2843	−0.3743	−0.7919	−0.4157	−0.8753	−0.4639	−0.97248
				0.05	−0.7224	−1.094	−0.7501	−1.1733	−0.7809	−1.2609	−0.3446	−0.7581	−0.3857	−0.8417	−0.4341	−0.93988
		1	0	−0.1	−0.4659	−0.8962	−0.4362	−0.9186	−0.401	−0.9397	−0.0024	−0.4826	0.0188	−0.5026	0.04017	−0.52849
				0	−0.4236	−0.8475	−0.3914	−0.8678	−0.3541	−0.8876	0.0587	−0.4141	0.0813	−0.433	0.10308	−0.45942
				0.05	−0.4006	−0.8216	−0.3669	−0.8407	−0.3284	−0.8597	0.0931	−0.3754	0.1165	−0.3939	0.13848	−0.42112
			0.05	−0.1	−0.4545	−0.88	−0.4239	−0.9005	−0.3878	−0.9197	0.0097	−0.4666	0.0315	−0.485	0.05371	−0.50901
				0	−0.4125	−0.8318	−0.3795	−0.8502	−0.3412	−0.868	0.0706	−0.3984	0.0939	−0.4157	0.11645	−0.4403
				0.05	−0.3897	−0.806	−0.3551	−0.8233	−0.3157	−0.8403	0.105	−0.3597	0.1291	−0.3767	0.15178	−0.40215
	10,000	0	0	−0.1	−1.2849	−1.8196	−1.4131	−2.0973	−1.5772	−2.4183	−1.0697	−1.615	−1.2005	−1.8875	−1.3483	−2.20535
				0	−1.2442	−1.765	−1.3717	−2.0428	−1.5387	−2.366	−1.0274	−1.5557	−1.1578	−1.8282	−1.3057	−2.14756
				0.05	−1.2233	−1.737	−1.3504	−2.0148	−1.519	−2.3392	−1.0057	−1.5251	−1.1359	−1.7976	−1.2839	−2.11786
			0.05	−0.1	−1.244	−1.7639	−1.3649	−2.0269	−1.5209	−2.3309	−1.0311	−1.5615	−1.155	−1.82	−1.295	−2.1215

			0	−1.2045	−1.7109	−1.3247	−1.9739	−1.4835	−2.2801	−0.9899	−1.5038	−1.1135	−1.7623	−1.2536	−2.06529
			0.05	−1.1842	−1.6836	−1.304	−1.9467	−1.4644	−2.2541	−0.9689	−1.474	−1.0922	−1.7326	−1.2324	−2.03639
	1	0	−0.1	−0.9804	−1.5711	−1.035	−1.7749	−1.1211	−2.0096	−0.6958	−1.2998	−0.7576	−1.4991	−0.8295	−1.73643
			0	−0.9344	−1.511	−0.9871	−1.7133	−1.0763	−1.9494	−0.6484	−1.2344	−0.709	−1.4323	−0.7802	−1.67009
			0.05	−0.9107	−1.48	−0.9624	−1.6815	−1.0534	−1.9185	−0.6241	−1.2006	−0.684	−1.3979	−0.7549	−1.6359
		0.05	−0.1	−0.9413	−1.5172	−0.9897	−1.708	−1.0692	−1.9279	−0.6577	−1.2473	−0.7137	−1.4344	−0.7791	−1.65744
			0	−0.8964	−1.4587	−0.943	−1.648	−1.0255	−1.8694	−0.6114	−1.1834	−0.6662	−1.3691	−0.7309	−1.59267
			0.05	−0.8733	−1.4285	−0.9189	−1.617	−1.0032	−1.8393	−0.5876	−1.1503	−0.6418	−1.3355	−0.7062	−1.55927
1	0	0	−0.1	−0.8496	−1.1884	−0.896	−1.2954	−1.0002	−1.4411	−0.6482	−0.9741	−0.7047	−1.0855	−0.7658	−1.21028
			0	−0.8248	−1.1507	−0.8707	−1.2569	−0.9781	−1.4057	−0.6242	−0.9355	−0.6806	−1.0464	−0.7417	−1.17125
			0.05	−0.8121	−1.1313	−0.8578	−1.2372	−0.9669	−1.3877	−0.6121	−0.9157	−0.6684	−1.0265	−0.7294	−1.15129
		0.05	−0.1	−0.8377	−1.1717	−0.8829	−1.276	−0.9854	−1.4186	−0.6371	−0.9584	−0.6924	−1.0672	−0.7521	−1.18911
			0	−0.8133	−1.1345	−0.8579	−1.238	−0.9636	−1.3837	−0.6135	−0.9203	−0.6686	−1.0287	−0.7283	−1.15057
			0.05	−0.8008	−1.1154	−0.8452	−1.2185	−0.9526	−1.3659	−0.6015	−0.9008	−0.6566	−1.009	−0.7162	−1.13087
	1	0	−0.1	−0.4935	−0.8729	−0.4691	−0.9066	−0.5078	−0.9766	−0.2253	−0.5894	−0.2185	−0.6328	−0.2098	−0.68286
			0	−0.465	−0.8301	−0.4395	−0.8621	−0.482	−0.9354	−0.1983	−0.546	−0.1909	−0.5883	−0.1818	−0.63766
			0.05	−0.4504	−0.8081	−0.4244	−0.8391	−0.4689	−0.9144	−0.1845	−0.5238	−0.1769	−0.5655	−0.1675	−0.61451
		0.05	−0.1	−0.4823	−0.857	−0.4569	−0.8884	−0.4944	−0.9559	−0.2143	−0.5739	−0.2064	−0.6152	−0.1966	−0.6628
			0	−0.4542	−0.8147	−0.4277	−0.8444	−0.469	−0.9153	−0.1876	−0.531	−0.1792	−0.5711	−0.1689	−0.61806
			0.05	−0.4398	−0.7929	−0.4128	−0.8217	−0.4561	−0.8945	−0.174	−0.509	−0.1653	−0.5486	−0.1549	−0.59515

Acknowledgements

The authors thank the reviewers for constructive comments which led to definite improvement in the paper.

References

[1] B.C. Sakiadis, Boundary layer behavior on continuous solid surfaces, AIChE J. 7 (1961) 26–28.
[2] L.J. Crane, Flow past a stretching plate, ZAMP 21 (1970) 645–647.
[3] N. Afzal, I.S. Varshney, The cooing of a low heat resistance stretching sheet moving through a fluid, Warme Stoffubertrag. 14 (1980) 289–293.
[4] W.H.H. Banks, Similarity solutions of the boundary layer equations for a stretching wall, J. Mec. Theor. Appl. 2 (1983) 375–392.
[5] C.K. Chen, M.I. Char, Heat transfer of a continuous stretching surface with suction or blowing, J. Math. Anal. Appl. 135 (1988) 568–580.
[6] P.S. Gupta, A.S. Gupta, Heat and mass transfer on a stretching sheet with suction or blowing, Can. J. Chem. Eng. 55 (1977) 744–746.
[7] J. Vleggaar, Laminar boundary layer behaviour on continuous accelerating surfaces, Chem. Eng. Sci. 32 (1977) 1517–1525.
[8] L.J. Grubka, K.M. Bobba, Heat transfer characteristics of a continuous stretching surface with variable temperature, ASME J. Heat Transfer 107 (1985) 248–250.
[9] T. Sarpakaya, Flow on non-Newtonian fluids in a magnetic field, AIChE J. 7 (1961) 324–328.
[10] H.I. Andersson, MHD flow of a visco-elastic fluid past a stretching surface, Acta Mech. 95 (1992) 227–230.
[11] P. Sam Lawrence, B. Nageswara Rao, Heat transfer in the MHD flow of a visco-elastic fluid over a stretching sheet, ZAMM 77 (1997) 317–319.
[12] M.S. Abel, A. Joshi, R.M. Sonth, Heat transfer in MHD visco-elastic fluid flow over a stretching surface, ZAMM 81 (2001) 691–698.
[13] M.K. Chowdhury, M.N. Islam, MHD free convection flow of visco-elastic fluid past an infinite vertical porous plate, Heat Mass Transfer 36 (2000) 439–447.
[14] S.K. Khan, M.S. Abel, M.R. Sonth, Visco-elastic MHD flow, heat and mass transfer over a porous stretching sheet with dissipation energy and stress work, Heat Mass Transfer 40 (2003) 47–57.
[15] M.S. Abel, N. Mahesha, Heat transfer in MHD visco-elastic fluid flow over a stretching sheet with variable thermal conductivity, non-uniform heat source and radiation, Appl. Math. Model. 32 (2008) 1965–1983.
[16] M.I. Char, Heat and mass transfer in a hydromagnetic flow of the visco-elastic fluid over a stretching sheet, J. Math. Anal. Appl. 186 (1994) 674–689.
[17] W.R. Schowalter, The application of boundary layer theory to power law pseudo plastic fluids: similar solutions, AIChE J. 6 (1960) 24–28.
[18] A. Acrious, M.J. Shah, E.E. Peterson, Momentum and heat transfer in laminar boundary layer flow on non-Newtonian fluids past external surfaces, AIChE J. 6 (1960) 312–316.
[19] S.Y. Lee, W.F. Ames, Similar solutions for non-Newtonian fluids, AIChE J. 12 (1966) 700–708.
[20] H.I. Andersson, K.H. Bech, B.S. Dandapat, Magnetohydrodynamic flow of a power law fluid over a stretching sheet, Int. J. Nonlinear Mech. 72 (4) (1992) 929–936.
[21] T.G. Howell, D.R. Jeng, K.J. Dewitt, Momentum and heat transfer on a continuous moving surface in a power law fluid, Int. J. Heat Mass Transfer 40 (1997) 1853–1861.
[22] M.A.A. Mahmoud, M.A.E. Mahmoud, Analytical solutions of hydromagnetic boundary layer flow of a non-Newtonian power law fluid past a continuously moving surface, Acta Mech. 181 (2006) 83–89.
[23] I.A. Hassanien, A.A. Abdullah, R.S.R. Gorla, Flow and heat transfer in a power law fluid over a non-isothermal stretching sheet, Math. Comput. Model. 28 (1998) 105–116.
[24] M.S. Abel, N. Mahesha, Effects of thermal buoyancy and variable thermal conductivity in a power law fluid past a vertical stretching sheet in the presence of non uniform heat source, Int. J. Nonlinear Mech. 44 (2009) 1–12.
[25] K. Vajraveleu, Flow and heat transfer in a saturated porous medium over a stretching surface, ZAMM 74 (1994) 605–614.
[26] K. Vajravelu, J. Nayfeh, Convective heat transfer at a stretching sheet, Acta Mech. 96 (1993) 47–54.
[27] T.C. Chaim, Heat transfer in a fluid with variable thermal conductivity over a linearly stretching sheet, Acta Mech. 129 (1998) 63–72.
[28] T.C. Chiam, Heat transfer with variable thermal conductivity in a stagnation point flow towards a stretching sheet, Int. Commun. Heat Mass Transfer 23 (1996) 239–248.
[29] P.S. Datti, K.V. Prasad, M.S. Abel, A. Joshi, MHD visco-elastic fluid flow over a non-isothermal stretching sheet, Int. J. Eng. Sci. 42 (2004) 935–946.
[30] K.V. Prasad, M.S. Abel, S.K. Khan, Momentum and heat transfer in visco-elastic fluid flow in a porous medium over a non-isothermal stretching sheet, Int. J. Numer. Meth. Heat Fluid Flow 10 (2000) 786–802.
[31] M.S. Abel, K.V. Prasad, M. Ali, Buoyancy force and thermal radiation effects in MHD boundary layer visco-elastic fluid flow over continuously moving stretching surface, Int. J. Therm. Sci. 44 (2005) 465–476.
[32] T.A. Savvas, N.C. Markatos, C.D. Papaspyrides, On the flow of non-Newtonian polymer solutions, Appl. Math. Model. 18 (1994) 14–21.
[33] K.R. Rajagopal, T.Y. Na, A.S. Gupta, Flow of a visco-elastic fluid over a stretching sheet, Rheol. Acta 23 (1984) 213–215.

[34] K.V. Prasad, Dulal Pal, P.S. Datti, MHD flow and heat transfer in the flow of a power law fluid over a non-isothermal stretching sheet, Commun. Nonlinear Sci. Numer. Simulat. 14 (2009) 2178–2189.

[35] M. Acharya, L.P. Singh, G.C. Dash, Heat and mass transfer over an accelerating surface with heat source in the presence of suction and blowing, Int. J. Eng. Sci. 37 (1999) 189–211.